Journal of Heat and Mass Transfer Research

Journal homepage: http://jhmtr.semnan.ac.ir

Semnan University

Coupled Integral Equations Approach in the Solution of Luikov Equations with Microwave Effect

Elenilson T. Cabral[a], Marcelo J. R. Souza[b], Emanuel N. Macêdo[a,c], Bruno M. Viegas[a], João N. N. Quaresma[*,a,c]

[a]*Graduate Program in Natural Resource Engineering in the Amazon, PRODERNA/ITEC/UFPA, Universidade Federal do Pará, 66075-110, Belém, PA, Brazil*

[b]*Wood Department, Institute of Natural Science and Technology, Universidade do Estado do Pará, CCNT/UEPA, Belém, PA, Brazil*

[c]*Process Simulation Laboratory, School of Chemical Engineering, FEQ/ITEC/UFPA, Universidade Federal do Pará, Campus Universitário do Guamá, Rua Augusto Corrêa, 01, 66075-110, Belém, PA, Brazil*

PAPER INFO

Paper history:
Received: 2019-12-18
Revised: 2020-05-02
Accepted: 2020-04-16

Keywords:
Drying;
Capillary-porous solid;
Microwaves;
Luikov equations;
Coupled integral equations approach.

ABSTRACT

The objective of this study was to present a mathematical modeling and solution approach for the drying process of spheroidal solids with the application of microwaves in capillary porous media based on Luikov equations, which was composed of a system of linear and coupled partial differential equations arising from the energy, mass and pressure balances inside the solid matrix. Additionally, the power generation term from the application of microwaves was added to this differential system. The solution to this problem was achieved through a Coupled Integral Equations Approach (CIEA), whose objective was the transformation of the initial PDE system into an ODEs one. A computer code was developed in the FORTRAN 90/95 programming language, which used the subroutine IVPAG from the IMSL library to solve the system of ODEs from the application of the CIEA. The results obtained were compared with other previously reported results in the literature to verify the methodology and subsequently showed satisfactory agreement with those results.

DOI: 10.22075/jhmtr.2020.19302.1264

1. Introduction

Studying the drying process of materials is an important topic that needs to be addressed carefully since, there are several reasons for carrying out the drying process of materials in order to provide a specific moisture level to meet legal and contractual requirements [1]. Such needs make drying an essential operation in various industries such as chemical, construction, pharmaceutical, food, pulp, and paper, among others [2]. But the evolution of the drying process has occurred at a slow pace and taken an extended period of time. However, in recent decades considerable progress has been made regarding our understanding of the fundamental aspects of this process, as well as more efficient dryer designs. Since 1978 a series of conferences have been held on the subject, reflecting the global interest in drying problems [3]. Additionally, numerous studies on mechanisms and mathematical formulations of heat and mass transfer in drying processes have been published, notably work by such pioneers such as De Vries [4], Luikov [5], and Whitaker [6].

There are several drying technologies used to reduce the humidity of numerous products of industrial, commercial, and social interest [2]. Additionally, techniques such as drying using hot air, cold drying, solar drying, spray drying, microwave drying, and vacuum drying, have various advantages and disadvantages that need to be evaluated before choosing a more specific technology. For example, the microwave technology has countless advantages over conventional methods, including minimizing the required heating time, exhibiting uniform temperature distribution, and providing higher efficiency, as well as offering improvements in product quality [7].

In addition, some studies on the use of microwave technology in certain drying materials have been performed. Budd and Hill [8] studied the heating of foodstuffs with flat geometry in a microwave oven, and the

[*] *Corresponding Author: João N. N. Quaresma, Graduate Program in Natural Resource Engineering in the Amazon, PRODERNA/ITEC/UFPA, Universidade Federal do Pará, 66075-110, Belém, PA, Brazil.*
Email: quaresma@ufpa.br

authors showed that the Lambert law could provide excellent results for drying problems under certain conditions. Fennel and Boldor [9] analyzed the drying of sorghum bagasse using microwave technology; parameters such as microwave power, reduction of the amount of moisture, and total efficiency of the system were examined. Song et al. [10] analyzed uniformity on the horizontal and vertical plane in a drying chamber with the temperature and humidity measured when using both hot air and microwave technologies. Furthermore, the effects of air temperature and microwave power on drying uniformity were investigated, and the results showed that an increase in warm air temperature and microwave power improved the drying rate and consistency in thermal load distribution. Makul et al. [11] analyzed the drying of Portland cement slurries using microwave technology. They examined the effects of microwave power and pressure level on the temperature, moisture content, and compressive strength of cement pastes. Si et al. [12] numerically and experimentally analyzed the drying of lignite using the MFBD technique, which combines the technological characteristics of the fluidized bed and microwave heating. Their numerical results were obtained with the FLUENT software and were shown to be in line with the experiments. Their results also showed that the fluidization quality and lignite drying rate increased with an increase in microwave power and air temperature. As it is known, drying constitutes a vital operation, where an adequate control on this process, minimizes loss of product quality and energy during the process, adding value to the final product. In this context, Kangarluei [13] studied the process of heat and mass transfer in industrial biscuit ovens, in which a mathematical model was presented with the heat transfer to the cookies occurring through radiation, convection, and conduction. The author concluded that the heat transfer distribution in the cookies was 69% by radiation, 28% by convection, and 3% by conduction.

On the other hand, numerous works presented in different areas of knowledge showed that the drying operation was present in several industrial segments and often determined the quality of the final product. Because of this, our study intended to model the drying process in capillary-porous solids using the Luikov equations [5] and considering the power generation term from the application of microwaves, which were obtained from the application of the Lambert law derived from simplifications in the Maxwell equations. Next, we proceeded with the solution of the problem by employing the Coupled Integral Equations Approach (CIEA) [14-27] to the system of equations describing the process of heat and mass transfer. The CIEA as an example of an Improved Lumped-Differential Formulation (ILDF) was used in solving the problems related to diffusion and convection. Generally, the results were satisfactory in solving problems involving heat transfer and mass in the drying of materials [16, 22]. It is worth noting that, the technique used in our study consisted of averaging the potentials in a particular direction whose gradients were relatively small. Subsequently, the integrals that emerged were handled by different formulations based on the Hermite formulas [28] for approximating integrals. The advantage of this technique was the elimination of one of the independent variables, while still retaining some information from the original system through the boundary conditions [17, 18].

Among researchers who have applied CIEA in this field, Cheroto et al. [16], can be cited, who used the CIEA methodology in a drying problem whose formulation made use of Luikov equations. Reis et al. [19] also used the CIEA in a one-dimensional thermal problem for wave propagation in a finite solid medium, and the methodology demonstrated that good results could be obtained for low values of the Biot number and relaxation time. Dantas et al. [22] applied the CIEA to reshape the two-dimensional drying problem in porous media, which was treated after using the Generalized Integral Transform Technique (GITT), with the use of hybrid tools in the formulation and solution of such problems and provided outstanding results. Naveira et al. [23] also used the CIEA to simplify an unsteady conjugated problem (convection-conduction) over plates with non-negligible thicknesses. In this work, the resulting equations were treated using the GITT, and the combination led to proposed amendments to the problem. The hybrid solution methodology proved accurate and robust from a numerical point of view. Sphaier and Jurumenha [24] used the CIEA to obtain an improved concentrated formulation and to analyze the heat and mass transfer in adsorbed gas storage discharge operations; the results were shown to be promising for the approximation $H_{1,1}/H_{0,0}$ to Fourier number (Fo) less than unity. In another study, Cardoso et al. [25] used the CIEA to reformulate and simplify the species conservation equations that govern the extraction of metals in processes for separating membranes; the simulation of the simplified mathematical model showed satisfactory results when compared with experimental results. Costa Junior and Naveira-Cotta [27] also used the CIEA to obtain a mathematical model of first-order ODEs for describing the concentration of local species in the synthesis of biodiesel. Their results showed that the application of the CIEA in combination with the Monte Carlo method with Markov Chain was a robust and efficient tool for analyzing reactive mass transfer systems.

Therefore, this work aimed to extend the concepts in the CIEA methodology and to analyze the problem of drying in spheroidal capillary porous media by solving the Luikov equations with a microwave source term. Extensive parametric analysis was performed for obtaining the numerical results, which were also compared with those available in the literature.

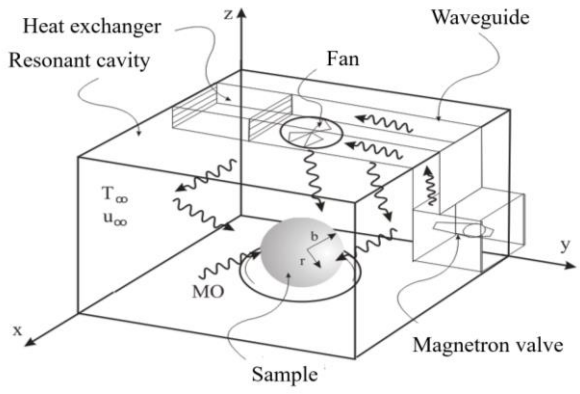

Figure 1. Microwave drying problem representation using porous solid spherical geometry.

2. Analysis

2.1. Mathematical formulation

The problem that was analyzed was that of simultaneous heat and mass transfer in a one-dimensional porous capillary spherical material exposed to electromagnetic radiation at the microwave frequency, with uniform initial temperature and moisture conditions under the influence of a pressure gradient. A sketch of the problem can be observed in Fig. 1.

The material that was dried was located at the center of a microwave applicator (resonant cavity type). The proposed model was based on the following assumptions:

1. The material to be dried was homogeneous, linear, isotropic and invariant;
2. The absorption of microwaves both by the cavity and the air was neglected. Also, it was considered that the walls of the waveguide were perfect conductors;
3. The solids to be dried and all materials used in the construction of the microwave applicator were non-magnetic;
4. The material absorbed the net power, provided by the generator valve microwave;
5. The electromagnetic field was uniformly distributed in the samples.

Therefore, the mathematical formulation of the problem in analysis was defined by the Luikov system of equations [29] with a coupled heat generation term, Q. This term represents the conversion of the electromagnetic wave energy into thermal energy [30]. Consequently, the dimensionless forms of the system equations were written as:

$$\frac{\partial\theta(R,\tau)}{\partial\tau} = K_{11}\nabla^2\theta + K_{12}\nabla^2\phi + K_{13}\nabla^2 P + Q, 0 < \mathrm{R} < 1, \tau > 0 \quad (1)$$

$$\frac{\partial\phi(R,\tau)}{\partial\tau} = K_{21}\nabla^2\theta + K_{22}\nabla^2\phi + K_{23}\nabla^2 P \quad (2)$$

$$\frac{\partial P(R,\tau)}{\partial\tau} = K_{31}\nabla^2\theta + K_{32}\nabla^2\phi + K_{33}\nabla^2 P \quad (3)$$

Equations (1) to (3) were subjected to the following initial and boundary conditions:

$$\theta(R,0) = 0, \phi(R,0) = 0, P(R,0) = 0, \quad 0 \le R \le 1 \quad (4a\text{-}c)$$

$$\frac{\partial\theta(0,\tau)}{\partial R} = 0, \frac{\partial\phi(0,\tau)}{\partial R} = 0, \frac{\partial P(0,\tau)}{\partial R} = 0, \quad \tau > 0 \quad (4d\text{-}f)$$

$$\frac{\partial\theta(1,\tau)}{\partial R} = Bi[1-\theta(1,\tau)] - (1-\varepsilon)Bi_m KoLu[1-\phi(1,\tau)],$$

$$\frac{\partial\phi(1,\tau)}{\partial R} = Bi_m^*[1-\phi(1,\tau)] - BiPn[\theta(1,\tau)-1] + \frac{BuLu_p}{KoLu}\frac{\partial P(1,\tau)}{\partial R}, \quad (4g\text{-}i)$$

$$P(1,\tau) = 0, \tau > 0$$

The Laplacian operator and the coefficients in Eqs. (1) to (3) are

$$\nabla^2 = \frac{1}{R^2}\frac{\partial}{\partial R}\left(R^2\frac{\partial}{\partial R}\right),$$

$$\mathrm{K}_{11} = 1 + \varepsilon\mathrm{KoLuPn},$$

$$\mathrm{K}_{12} = -\varepsilon\mathrm{KoLuPn},$$

$$\mathrm{K}_{13} = \varepsilon\mathrm{BuLu_p},$$

$$\mathrm{K}_{21} = -\mathrm{LuPn},$$

$$\mathrm{K}_{22} = \mathrm{Lu},$$

$$\mathrm{K}_{23} = -\frac{\mathrm{BuLu_p}}{Ko},$$

$$\mathrm{K}_{31} = -\varepsilon\frac{Ko\mathrm{LuPn}}{Bu},$$

$$\mathrm{K}_{32} = \varepsilon\frac{Ko\mathrm{Lu}}{Bu},$$

$$\mathrm{K}_{33} = (1-\varepsilon)\mathrm{Lu_p} \quad (5a\text{-}j)$$

Where the dimensionless quantities used in Eqs. (1) to (4) are defined as

$$R = \frac{r}{b}, \tau = \frac{\alpha t}{b^2}, \theta(R,\tau) = \frac{T(r,t)-T_0}{T_\infty - T_0},$$

$$\phi(R,\tau) = \frac{u_0 - u(r,t)}{u_0 - u_\infty},$$

$$P(R,\tau) = \frac{p(r,t)-p_0}{p_0},$$

$$Bi = \frac{h\,b}{k},$$

$$Bi_m = \frac{h_m\,b}{k_m},$$

$$Bi_m^* = Bi_m[1-(1-\varepsilon)KoLuPn],$$

$$Bu = \frac{\lambda c_p\,p_0}{c(T_\infty - T_0)},$$

$$Ko = \frac{\lambda(u_0 - u_\infty)}{c(T_\infty - T_0)},$$

$$Lu = \frac{\alpha_m}{\alpha},$$

$$Lu_p = \frac{\alpha_p}{\alpha},$$

$$Pn = \frac{\delta(T_\infty - T_0)}{(u_0 - u_\infty)}, \quad (6a\text{-}p)$$

$$Q = Q_0 \frac{\left[e^{-\Lambda(1-R)} - e^{-\Lambda(1+R)}\right]}{R^2},$$

$$Q_0 = \frac{\alpha_a P_{0i}}{2\pi(T_\infty - T_0)k},$$

$$\Lambda = 2\alpha_a b$$

The various quantities that appear in Eqs. (6) are labeled in the Nomenclature Section.

2.2. Solution methodology

The solution methodology involved the integration of Eqs. (1) to (3) in the R-direction that were presumed to have small gradients; the potential and respective derivatives at the boundaries were evaluated through the Hermite integration formulas [28]. This methodology is known as a Coupled Integral Equations Approach (CIEA) [22,25].

2.2.1. Hermite approximation

Hermite [28] developed a way to approach an integral, using the values of integration and its derivatives within the limits of integration, in the form:

$$\int_{x_{i-1}}^{x_i} f(x)dx = \sum_{\nu=0}^{\alpha} C_\nu f_{i-1}^{(\nu)} + \sum_{\nu=0}^{\beta} D_\nu f_i^{(\nu)} \qquad (7)$$

Where f(x) and its derivatives $f^{(\nu)}(x)$ are defined for all $x \in (x_{i-1}, x_i)$. However, it is assumed that the numerical values of $f^{(\nu)}(x_{i-1}) \equiv f_{i-1}^{(\nu)}$ for $\nu = 0, 1, 2,...,\alpha$ and $f^{(\nu)}(x_i) \equiv f_i^{(\nu)}$ for $\nu = 0,1,2,...,\beta$ are available at the extremes of the range, so that the integral for f(x) is expressed as a linear combination of $f(x_{i-1})$, $f(x_i)$ and its derivatives $f^{(\nu)}(x_{i-1})$ to order $\nu = \alpha$ and $f^{(\nu)}(x_i)$ to order $\nu = \beta$. This is called the $H_{\alpha,\beta}$ approach. A systemized derivation for arbitrary α and β was presented by Mennig et al. [31]. The resulting expression for the $H_{\alpha,\beta}$ approach is given by:

$$\int_{x_{i-1}}^{x_i} f(x)dx = \sum_{\nu=0}^{\alpha} C_\nu(\alpha,\beta) h_i^{\nu+1} f_{i-1}^{(\nu)} + \sum_{\nu=0}^{\beta} C_\nu(\beta,\alpha)(-1)^\nu h_i^{\nu+1} f_i^{(\nu)} + O(h_i^{\alpha+\beta+3}) \qquad (8)$$

Where

$$C_\nu(\alpha,\beta) = \frac{(\alpha+1)!(\alpha+\beta+1-\nu)!}{(\nu+1)!(\alpha-\nu)!(\alpha+\beta+2)!}, \qquad (9a,b)$$

$$h_i = x_i - x_{i-1}$$

In this analysis, we consider the following approximation:

$$H_{1,1} \rightarrow \int_0^h f(x)dx \cong \frac{h}{2}[f(0) + f(h)] + \frac{h^2}{12}[f'(0) - f'(h)] \qquad (10)$$

Equation (10) corresponds to the integration of the corrected trapezoidal rule.

2.2.2. Classical approximation

In this approach, the gradients within the body along the radial direction are neglected. One can then obtain the expressions for the temperature at the surface of the sphere, the moisture content, and the pressure gradient from the approximation of these potentials by the correspondent average potentials, i.e., by the integration of the original PDEs over the independent R-variable within the domain. Such a procedure results in a simplified formulation for the equations by eliminating the spatial dependence. Therefore, one defines the average potentials as follows:

$$\tilde{\theta}(\tau) = 3\int_0^1 R^2\theta(R,\tau)\,dR,$$

$$\tilde{\phi}(\tau) = 3\int_0^1 R^2\phi(R,\tau)\,dR, \qquad (11a\text{-}c)$$

$$\tilde{P}(\tau) = 3\int_0^1 R^2 P(R,\tau)\,dR$$

The temperature, moisture, and pressure fields are coupled by the boundary conditions given by Eqs. (4g, h) at R=1. Therefore, it is necessary to determine these potentials at this specific position. However, it is known that in the classical approach, the temperature and moisture potentials in the solid surface are approximated by the average potentials given by Eqs. (11), i.e.:

$$\theta(1,\tau) \cong \tilde{\theta}(\tau), \phi(1,\tau) \cong \tilde{\phi}(\tau) \qquad (12a,b)$$

Thus, by substituting Eqs. (12) into Eqs. (4g, h), one obtains

$$\frac{\partial\theta(1,\tau)}{\partial R} = Bi\left[1 - \tilde{\theta}(\tau)\right] - (1-\varepsilon)Bi_m KoLu\left[1 - \tilde{\phi}(\tau)\right],$$

$$\frac{\partial\phi(1,\tau)}{\partial R} = Bi_m^*\left[1 - \tilde{\phi}(\tau)\right] - BiPn[\tilde{\theta}(\tau) - 1] + \frac{BuLu_p}{KoLu}\frac{\partial P(1,\tau)}{\partial R} \qquad (13a, b)$$

To determine $\partial P(1,\tau)/\partial R$, the definition for the pressure average given by Eq. (11c) was used, along with the Hermite formula $H_{1,1}$ given by Eq. (10), to yield

$$\frac{1}{3}\tilde{P}(\tau) = \int_0^1 R^2 P(R,\tau)\,dR \cong \frac{1}{2}[(R^2P)|_{R=0} + (R^2P)|_{R=1}] + \frac{1}{12}\left[\left.\frac{\partial(R^2P)}{\partial R}\right|_{R=0} - \left.\frac{\partial(R^2P)}{\partial R}\right|_{R=1}\right] \qquad (14)$$

$$= \frac{1}{2}[P(1,\tau)] + \frac{1}{12}\left[-2P(1,\tau) - \frac{\partial P(1,\tau)}{\partial R}\right]$$

Using boundary condition (4i) into Eq. (14), one obtains the following expression:

$$\frac{\partial P(1,\tau)}{\partial R} = -4\tilde{P}(\tau) \tag{15}$$

The next step is to perform the integration of Eqs. (1) to (3) in the R-direction in the domain R ∈ [0,1]. Next, the definitions of average potentials in Eqs. (11) are used, to generate the following system of ODEs for the classical approach:

$$\frac{d\tilde{\theta}(\tau)}{d\tau} = 3\left[K_{11}\frac{\partial\theta(1,\tau)}{\partial R} + K_{12}\frac{\partial\phi(1,\tau)}{\partial R} + K_{13}\frac{\partial P(1,\tau)}{\partial R} + Q_0\frac{1-2e^{-\Lambda}+e^{-2\Lambda}}{\Lambda}\right] \tag{16}$$

$$\frac{d\tilde{\phi}(\tau)}{d\tau} = 3\left[K_{21}\frac{\partial\theta(1,\tau)}{\partial R} + K_{22}\frac{\partial\phi(1,\tau)}{\partial R} + K_{23}\frac{\partial P(1,\tau)}{\partial R}\right] \tag{17}$$

$$\frac{d\tilde{P}(\tau)}{d\tau} = 3\left[K_{31}\frac{\partial\theta(1,\tau)}{\partial R} + K_{32}\frac{\partial\phi(1,\tau)}{\partial R} + K_{33}\frac{\partial P(1,\tau)}{\partial R}\right] \tag{18}$$

With initial conditions given by:

$$\tilde{\theta}(0) = 0, \tilde{\phi}(0) = 0, \tilde{P}(0) = 0 \tag{19a-c}$$

The derivatives $\partial\theta(1,\tau)/\partial R$, $\partial\phi(1,\tau)/\partial R$ and $\partial P(1,\tau)/\partial R$ that appear in Eqs. (16) to (18) are given by Eqs. (13a, b) and (15), respectively.

2.2.3. $H_{1,1}$ - $H_{1,1}$ Approximation

This methodology first starts by searching for a solution for the integral of $\partial\theta/\partial R$ as follows:

$$\int_0^1 \frac{\partial\theta(R,\tau)}{\partial R}\,dR = \theta(1,\tau) - \theta(0,\tau) \tag{20}$$

Solving the integral of Eq. (20) by $H_{1,1}$ approximation, presented in Eq. (10), and using boundary condition (4d), then:

$$\theta(1,\tau) - \theta(0,\tau) = \frac{1}{2}\frac{\partial\theta(1,\tau)}{\partial R} + \frac{1}{12}\left[\frac{\partial^2\theta(0,\tau)}{\partial R^2} - \frac{\partial^2\theta(1,\tau)}{\partial R^2}\right] \tag{21}$$

Now, the objective is to find relationships for the second partial derivatives in Eq. (21), and this is done by making use of the following integral:

$$\int_0^1 R^3\frac{\partial\theta(R,\tau)}{\partial R}\,dR = \theta(1,\tau) - 3\int_0^1 R^2\theta(R,\tau)\,dR = \theta(1,\tau) - \tilde{\theta}(\tau) \tag{22}$$

Using the $H_{1,1}$ approximation to solve the integral in Eq. (22) and equalizing the results, one finds

$$\frac{\partial^2\theta(1,\tau)}{\partial R^2} = 12\left[\tilde{\theta}(\tau) - \theta(1,\tau)\right] + 3\frac{\partial\theta(1,\tau)}{\partial R} \tag{23}$$

Substituting Eq. (23) into Eq. (21), the result is:

$$\frac{\partial^2\theta(0,\tau)}{\partial R^2} = 12[\tilde{\theta}(\tau) - \theta(0,\tau)] - 3\frac{\partial\theta(1,\tau)}{\partial R} \tag{24}$$

Similarly, we obtain the following relations for the moisture and pressure fields:

$$\frac{\partial^2\phi(1,\tau)}{\partial R^2} = 12[\tilde{\phi}(\tau) - \phi(1,\tau)] + 3\frac{\partial\phi(1,\tau)}{\partial R} \tag{25}$$

$$\frac{\partial^2\phi(0,\tau)}{\partial R^2} = 12[\tilde{\phi}(\tau) - \phi(0,\tau)] - 3\frac{\partial\phi(1,\tau)}{\partial R} \tag{26}$$

$$\frac{\partial^2 P(1,\tau)}{\partial R^2} = 0 \tag{27}$$

$$\frac{\partial^2 P(0,\tau)}{\partial R^2} = 12[\tilde{P}(\tau) - P(0,\tau)] - 3\frac{\partial P(1,\tau)}{\partial R} \tag{28}$$

Where,

$$\frac{\partial\theta(1,\tau)}{\partial R} = Bi[1-\theta(1,\tau)] - (1-\varepsilon)Bi_m KoLu[1-\phi(1,\tau)],$$
$$\frac{\partial\phi(1,\tau)}{\partial R} = Bi_m^*[1-\phi(1,\tau)] - BiPn[\theta(1,\tau)-1] + \frac{BuLu_p}{KoLu}\frac{\partial P(1,\tau)}{\partial R},$$
$$\frac{\partial P(1,\tau)}{\partial R} = -4\tilde{P}(\tau) \tag{29a-c}$$

Next, we use Eq. (1) to determine the potentials $\theta(1,\tau)$ and $\theta(0,\tau)$. For this purpose, we take the limit of Eq. (1) when R→0 and R→1, respectively. Nonetheless, a problem arises in doing so, given that a singularity occurs in the term of energy generation, Q, in Eq. (1), when R→0. Some studies in this field that used the Lambert law, have avoided the problems inherent to this singularity by disregarding the energy generation term in their mathematical formulation when R = 0 [32]. In our analysis, we used the assumption made by Chen et al. [33] in which R is always ≥ *s*, with *s* being an infinitely small positive number. Starting from this assumption, Q→0 when R→*s*, the following expression results:

$$\frac{d\theta(0,\tau)}{d\tau} = 3\left[K_{11}\frac{\partial^2\theta(0,\tau)}{\partial R^2} + K_{12}\frac{\partial^2\phi(0,\tau)}{\partial R^2} + K_{13}\frac{\partial^2 P(0,\tau)}{\partial R^2}\right] \tag{30}$$

Applying the limit in Eq. (1) when R→1, it results:

$$\frac{d\theta(1,\tau)}{d\tau} = K_{11}\left[2\frac{\partial\theta(1,\tau)}{\partial R} + \frac{\partial^2\theta(1,\tau)}{\partial R^2}\right] + K_{12}\left[2\frac{\partial\phi(1,\tau)}{\partial R} + \frac{\partial^2\phi(1,\tau)}{\partial R^2}\right] + 2K_{13}\frac{\partial P(1,\tau)}{\partial R} + Q_0(1-e^{-2\Lambda}) \tag{31}$$

A similar procedure was also applied to the moisture and pressure fields. By making $\theta(0,\tau)\equiv\theta_0(\tau)$, $\theta(1,\tau)\equiv\theta_1(\tau)$, $\phi(0,\tau)\equiv\phi_0(\tau)$, $\phi(1,\tau)\equiv\phi_1(\tau)$ and $P(0,\tau)\equiv P_0(\tau)$, we therefore

as a result, obtain the following system of ODEs for the $H_{1,1}$ approach with their respective initial conditions:

$$\frac{d\tilde{\theta}(\tau)}{d\tau} = 3\left[K_{11}\frac{\partial\theta(1,\tau)}{\partial R} + K_{12}\frac{\partial\phi(1,\tau)}{\partial R} + K_{13}\frac{\partial P(1,\tau)}{\partial R} + Q_0\frac{1-2e^{-\Lambda}+e^{-2\Lambda}}{\Lambda}\right] \quad (32)$$

$$\frac{d\tilde{\phi}(\tau)}{d\tau} = 3\left[K_{21}\frac{\partial\theta(1,\tau)}{\partial R} + K_{22}\frac{\partial\phi(1,\tau)}{\partial R} + K_{23}\frac{\partial P(1,\tau)}{\partial R}\right] \quad (33)$$

$$\frac{d\tilde{P}(\tau)}{d\tau} = 3\left[K_{31}\frac{\partial\theta(1,\tau)}{\partial R} + K_{32}\frac{\partial\phi(1,\tau)}{\partial R} + K_{33}\frac{\partial P(1,\tau)}{\partial R}\right] \quad (34)$$

$$\frac{d\theta_0(\tau)}{d\tau} = 3\left[K_{11}\frac{\partial^2\theta(0,\tau)}{\partial R^2} + K_{12}\frac{\partial^2\phi(0,\tau)}{\partial R^2} + K_{13}\frac{\partial^2 P(0,\tau)}{\partial R^2}\right] \quad (35)$$

$$\frac{d\theta_1(\tau)}{d\tau} = K_{11}\left[2\frac{\partial\theta(1,\tau)}{\partial R} + \frac{\partial^2\theta(1,\tau)}{\partial R^2}\right] + K_{12}\left[2\frac{\partial\phi(1,\tau)}{\partial R} + \frac{\partial^2\phi(1,\tau)}{\partial R^2}\right] + 2K_{13}\frac{\partial P(1,\tau)}{\partial R} + Q_0(1-e^{-2\Lambda}) \quad (36)$$

$$\frac{d\phi_0(\tau)}{d\tau} = 3\left[K_{21}\frac{\partial^2\theta(0,\tau)}{\partial R^2} + K_{22}\frac{\partial^2\phi(0,\tau)}{\partial R^2} + K_{23}\frac{\partial^2 P(0,\tau)}{\partial R^2}\right] \quad (37)$$

$$\frac{d\phi_1(\tau)}{d\tau} = K_{21}\left[2\frac{\partial\theta(1,\tau)}{\partial R} + \frac{\partial^2\theta(1,\tau)}{\partial R^2}\right] + K_{22}\left[2\frac{\partial\phi(1,\tau)}{\partial R} + \frac{\partial^2\phi(1,\tau)}{\partial R^2}\right] + 2K_{23}\frac{\partial P(1,\tau)}{\partial R} \quad (38)$$

$$\frac{dP_0(\tau)}{d\tau} = 3\left[K_{31}\frac{\partial^2\theta(0,\tau)}{\partial R^2} + K_{32}\frac{\partial^2\phi(0,\tau)}{\partial R^2} + K_{33}\frac{\partial^2 P(0,\tau)}{\partial R^2}\right] \quad (39)$$

$$\tilde{\theta}(0) = 0, \tilde{\phi}(0) = 0, \tilde{P}(0) = 0 \quad (40a\text{-}c)$$

$$\theta_0(0) = 0, \theta_1(0) = 0, \phi_0(0) = 0, \phi_1(0) = 0, P_0(0) = 0 \quad (40d\text{-}h)$$

The various first and second derivatives that appear in Eqs. (32) to (39) are given by Eqs. (23) to (29).

3. Results

Numerical results were computed for the average potentials and at the sphere surface as a function of the time variable, t. For the solution of the coupled system of ODEs, the DIVPAG subroutine from the IMSL Library [34] was used in a computer code developed in the Fortran 90/95 programming language.

First, the verification of the computer code was performed for two cases (Cases 1 and 2), which considered that there was no power generation in the solid to be dried by microwaves. The values for the dimensionless groups used are listed in Table 1.

In Case 1, the consideration was made that the influence of the pressure gradient was negligible, as discussed by Conceição et al. [29]. Therefore, to make nulls the pressure terms in the Luikov equations, the Bulygin (the ratio between the filtration and the sensible heat) and the Luikov filtration (the ratio between the filtration ability and the energy diffusivity in the porous matrix) numbers were considered as $Bu \to \infty$ and $Lu_p \to 0$, respectively.

The results for this case are shown in Table 2. These results were then compared with the values obtained by Conceição et al. [29] for dimensionless times 0.3, 0.5, 0.7, and 1 to verify the present methodology. From Table 2, one may observe a good correlation between the results of the Classical and $H_{1,1}$ approaches for the temperature field. It is clear, however, that for the moisture field, there was considerable difference between the results obtained from the two approaches. When comparing these results with those obtained in reference [29], we also noticed a sensible difference with a maximum relative deviation of 18.7% and 3.90% for the moisture field in the Classical and $H_{1,1}$ strategies, respectively. This difference was because the proposed approaches in this study had limitations for Biot numbers: $Bi > 0.1$ and $Bi_m > 0.1$. Note, however, in Figs. 2a and 2b that the approaches solution had a tendency compatible with the physics of the problem. That was, it tended to balance the temperature and moisture conditions of the medium.

Case 2 was used to verify the methodology employed, like Case 1, and, additionally, to evaluate the influence of the pressure gradient. The results obtained for the dimensionless times 0.3, 0.5, 0.7, and 1 can be seen in Table 3. Also, from this table, we observed that the maximum relative deviations of 70.9% (Classical approach) and 18.5% ($H_{1,1}$ strategy) were found for the pressure distribution. The results for Case 2 show that the $H_{1,1}$ approach provided a prediction with good agreement when compared with the results obtained by Conceição et al. [29] for the temperature, moisture, and pressure fields as a function of the time variable, as can be seen in Fig. 3.

Table 1. Dimensionless parameters used for the verification of computer code [29].

Case	Dimensionless Parameters							
	ε	Bi	Bi_m	Bu	Ko	Lu	Lu_p	Pn
1	0.25	5.0	2.5	∞	1.2	0.3	0	0.25
2	0.25	5.0	2.5	0.001	1.2	0.3	100	0.25

Table 2. Results for Case 1.

	$\theta(1,\tau)$				
τ	Classical Approximation	Relative Deviation (%)	$H_{1,1}$ Approximation	Relative Deviation (%)	Conceição *et al.* [29]
0.3	0.88342	0.927	0.88034	0.575	0.87531
0.5	0.93081	0.337	0.93260	0.530	0.92768
0.7	0.95614	0.556	0.95565	0.505	0.95085
1.0	0.97768	0.879	0.97259	0.354	0.96916
	$\phi(1,\tau)$				
τ	Classical Approximation	Relative Deviation (%)	$H_{1,1}$ Approximation	Relative Deviation (%)	Conceição *et al.* [29]
0.3	0.49084	18.7	0.60326	0.0911	0.60381
0.5	0.67535	4.15	0.73208	3.90	0.70458
0.7	0.79299	2.10	0.80378	3.49	0.77667
1.0	0.89460	4.88	0.87053	2.07	0.85291

Table 3. Results for Case 2.

	$\theta(1,\tau)$				
τ	Classical Approximation	Relative Deviation (%)	$H_{1,1}$ Approximation	Relative Deviation (%)	Conceição *et al.* [29]
0.3	0.88342	1.40	0.87367	0.276	0.87126
0.5	0.93081	0.672	0.92832	0.403	0.92459
0.7	0.95614	0.716	0.95395	0.486	0.94934
1.0	0.97768	0.855	0.97312	0.385	0.96939
	$\phi(1,\tau)$				
τ	Classical Approximation	Relative Deviation (%)	$H_{1,1}$ Approximation	Relative Deviation (%)	Conceição *et al.* [29]
0.3	0.49084	15.5	0.57054	1.79	0.58095
0.5	0.67535	2.30	0.71568	3.53	0.69125
0.7	0.79299	2.70	0.79970	3.57	0.77214
1.0	0.89460	4.47	0.87577	2.27	0.85635
	P(0,τ)				
τ	Classical Approximation	Relative Deviation (%)	$H_{1,1}$ Approximation	Relative Deviation (%)	Conceição *et al.* [29]
0.3	0.28694	46.8	0.63931	18.5	0.53955
0.5	0.18296	58.4	0.41489	5.66	0.43980
0.7	0.11666	64.2	0.28667	12.1	0.32618
1.0	0.05940	70.9	0.17564	14.1	0.20437

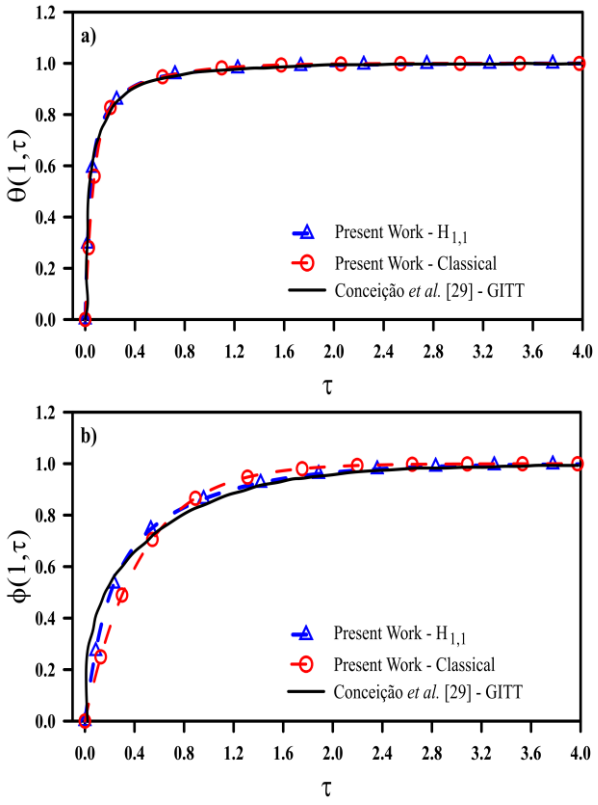

Figure 2. Development of the potentials as a function of the time variable for Case 1:
(a) temperature profile; (b) moisture profile.

The remarks made for Case 1 can also be applied to Case 2. It can be said that the pressure gradient did not interfere significantly in the temperature distribution by comparing the two cases. While for the moisture field, Fig. 3b, the pressure gradient caused a considerable reduction in the moisture content, especially in the first instance, as shown in Table 2 and 3. This behavior was expected, since it was known that for intense drying processes the pressure gradient became significant and contributed to a faster reduction of the moisture content.

The high-value Lu_p for this case showed that the ability of the porous solid in filtering (extruding) the moisture to its surface was more significant than its ability to impart thermal energy, thus contributing mainly to the change in the moisture profile.

From the observation of Fig. 3c, it is concluded that the results of Classical and $H_{1,1}$ approaches had a physical behavior compatible with that seen by Conceição et al. [29]. Moreover, there was a pressure increase in the first moments after microwave exposure, explained by an increase in the amount of steam in the porous matrix due to the heat transfer process. In the course of the drying process, the ability of the porous capillary solid to transfer out the steam-gas mixture increased, causing a decrease in the pressure field.

It can be concluded from the analysis of Cases 1 and 2 that the $H_{1,1}$ approach provided satisfactory results when compared to those offered by the methodology of GITT employed by Conceição et al. [29] in their work. As the

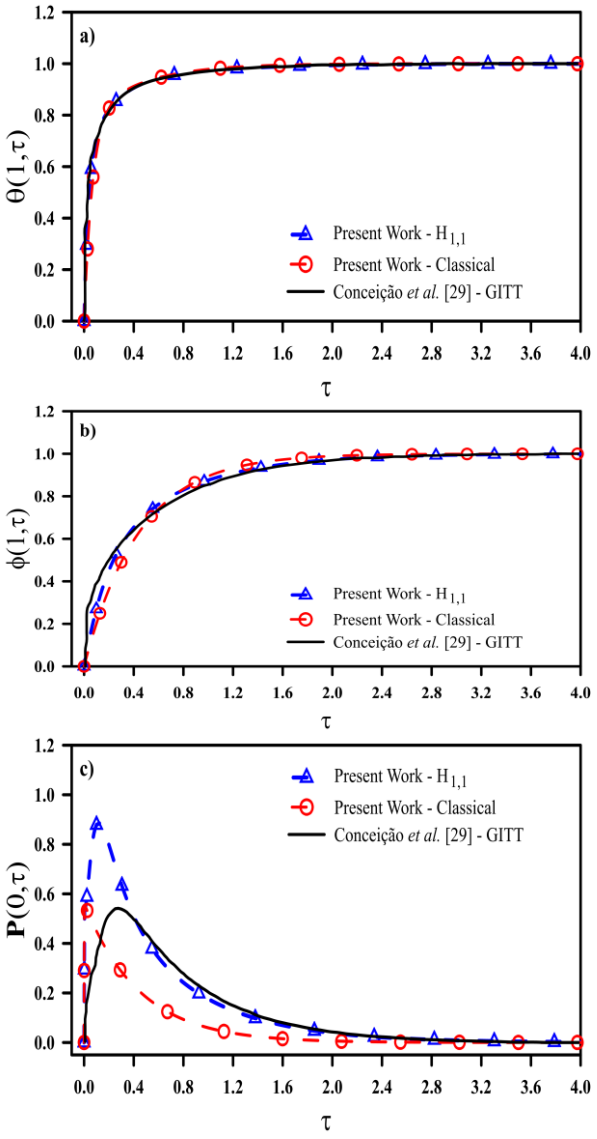

Figure 3. Development of the potentials as a function of the time variable for Case 2:
(a) temperature profile; (b) moisture profile; (c) pressure profile.

Classical approach predicts an average potential for the entire domain within the porous medium, its accuracy fails at the points R = 0 and R = 1. On the other hand, because the $H_{1,1}$ approach considers additional equations to compute the potentials at the boundaries; therefore, as a consequence, its precision is improved.

Moving forward, we proposed to simulate the microwave drying of spherical materials, keeping the values of dimensionless groups for Case 2 and considering processing the materials in a microwave oven such as the one shown in Fig. 1, operating at a frequency equal to 2.45 GHz. Thus, two other cases (Cases 3 and 4) were addressed in this analysis.

Additionally, in all these cases, the dimensionless excitation time of the material for microwave, τ_{exc}, was

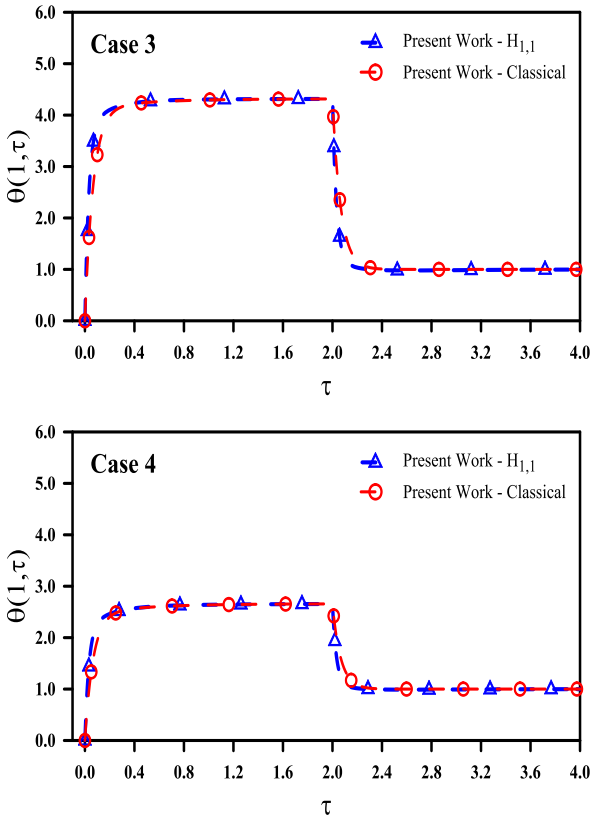

Figure 4. Temperature distribution at R = 1 for Cases 3 and 4.

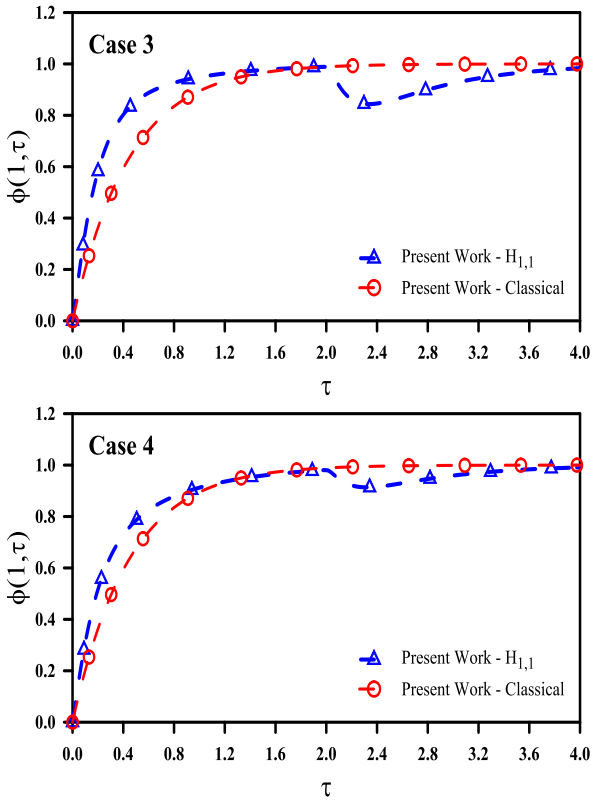

Figure 5. Moisture distribution at R = 1 for Cases 3 and 4.

Table 4. Values considered in the analysis of microwave drying.

Case	Dimensionless Parameters	
	Λ	Q
3	6	100
4	6	50

equal to half the dimensionless drying processing time of the solid, i.e., τ_{exc}=2, since, it was observed from the results obtained that it reached a steady-state for the temperature field close to it. However, it is well known that the dimensionless moisture potential changes until it becomes a new steady-state.

The analysis was based on the values of dimensionless power, Q, which are shown in Table 4. These results obtained for these cases for the temperature field at R = 1 can be seen in Figs. 4.

In an analysis of Cases 3 and 4, following a decrease in the dimensionless power, there is also a decrease in the maximum dimensionless temperature measured on the surface of the material. Such an observation was already expected because the amount of energy provided was reduced every time. There was a sharp decrease in potential temperature for τ=2, caused by the cessation of the supply of electromagnetic energy to the material. Finally, there was good agreement between the results of Classical and $H_{1,1}$ approaches for the dimensionless temperature potential at R = 1.

Results for the moisture potential are shown in Fig. 5 for Cases 3 and 4. It can be seen from the analysis of Fig. 5 that the moisture behavior was consistent with Cases 3 and 4. With the decrease of the power applied, the maximum temperature was lower, but the final moisture content was the same for both cases. This fact indicates that the conditions of Case 3 were more advantageous; however, a more detailed study of the properties of the material to be dried must be conducted to verify that the solid will not undergo degradation due to the effect of high power.

Furthermore, results were generated for temperature and moisture potentials as a function of dimensionless time, τ, when R = 0, as shown in Figs. 6. First, it was found that for the temperature potential at R = 0, there was no agreement between the results of the Classical and $H_{1,1}$ approaches. This could be explained again by the assumption that the Classical approach considered an average profile for the potentials across the material domain and failed to predict the distributions in cases with a high characteristic length, besides the fact that Bi and Bi_m values were higher than 0.1.

By changing the dimensionless power, one may observe the same behavior registered for the temperature potential at R = 1, with the proper proportions.

In Figs. 5 and 7, we show the analysis of the drying

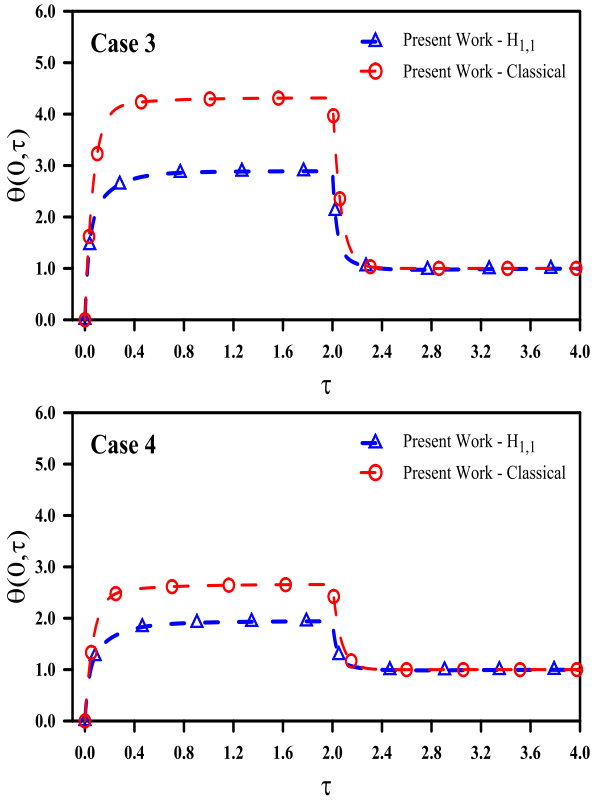

Figure 6. Temperature distribution at R = 0 for Cases 3 and 4.

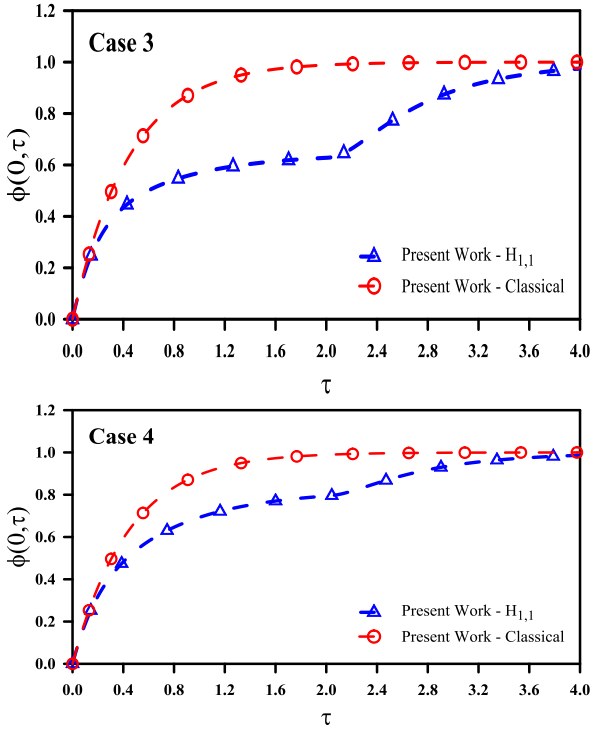

Figure 7. Moisture distribution at R = 0 for Cases 3 and 4.

process behavior after the excitation period of the material by the microwave, since it is known that when the internal power generation ceases, the content tends towards thermal equilibrium with the environment, even if the drying process continues.

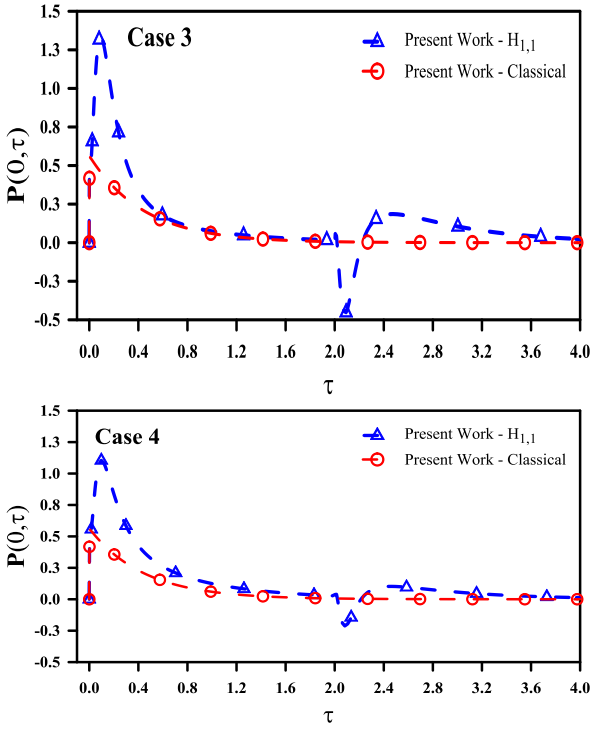

Figure 8. Pressure distribution at R = 0 for Cases 3 and 4.

For the moisture potential on the surface (Fig. 5), there was a smooth fall at the time τ=2 due to the decrease of the material temperature, which was caused by some of the vapor leaving the interior of the solid to condense on the surface. However, the moisture present inside the body continued diffusing to the surface, and this again resulted in increasing the moisture potential until it reached a new equilibrium with the environment.

Finally, Fig. 8 shows the pressure potential for Cases 3 and 4. Note the substantial similarity to the behavior of the potential pressure as for Case 2 until time τ=2, when the excitation period ended. The gradient became inverted after this moment.

Conclusion

In this study, the applicability of the Coupled Integral Equations Approach (CIEA) was investigated in a drying problem involving capillary-porous spherical materials with and without the use of microwaves, in which the heat and mass transfer model considered was proposed by Luikov equations.

The results were compared to those presented by Conceição et al. [29] to verify the employed methodology. These results showed that the CIEA method, specifically the $H_{1,1}$ approach, exhibited an acceptable behavior for drying problems despite its simplicity compared to other methods, such as the GITT approach.

Results were also proposed for a drying problem by applying microwaves, which considered the power generating term derived from the Lambert law whose applicability occurs in semi-infinite media, even if these results needed validation. Results for temperature,

moisture, and pressure potentials were physically adequate. The results indicated an acceptable use potential for the CIEA approach in simulating a fast-drying method, using a microwave in spherical geometry.

It is noteworthy that the greatest difficulty in working with the heat and mass transfer equations in drying problems modeled by Luikov equations is in obtaining the thermo-physical properties of various materials. Such complexity is justified in the physically interpreting of the parameters presented, leading to a few theoretical and experimental studies that used such a model.

For a more detailed study of the electromagnetic field distribution in various materials, the use of Maxwell field equations is recommended for future work.

It follows, therefore, that the objective of this work was achieved satisfactorily because a detailed analysis was performed concerning the solid spheroidal drying phenomenon by applying microwaves.

Finally, as an extension of the present work, we can point out that it is possible to adopt the GITT methodology as in the reference [29], with just one single term in the eigenfunction expansions, for the evaluation of the average potentials. Such an approach could offer an approximate competitive solution based only on the resolution of a reduced model based on ODEs, as stated in the work of Cotta and Ramos [35].

Nomenclature

b	sphere radius
Bi	Biot number
Bi_m	Biot for mass transfer number
Bi_m^*	modified Biot number for mass transfer
Bu	Bulygin number
c	specific heat
cp	coefficient of humid air capacity
h	heat transfer coefficient
h_m	mass transfer coefficient
k	thermal conductivity
k_m	moisture conductivity
Ko	Kossovich number
K_{ij}	coefficients defined by Eqs. (5b-j) (i=1,2,3; j=1,2,3)
Lu	Luikov number
Lu_p	Luikov for filtration number
p, P	pressure fields, dimensional and dimensionless, respectively
Pn	Posnov number
p_0	initial pressure distribution in the medium
P_{0i}	incident microwave power on the sphere
P_0	pressure at R=0
$\tilde{P}$	average pressure
Q	microwave power absorption
r, R	radial coordinates, dimensional and dimensionless, respectively
t	time variable
T	temperature field
T_∞	temperature of the surrounding air
T_0	initial temperature in the medium
u	moisture field
u_∞	moisture content of the surrounding air
u_0	initial moisture content in the medium

Greek letters

α	thermal diffusivity
α_a	attenuation constant
α_m	moisture diffusivity
α_p	vapor diffusion coefficient for filtration motion
δ	thermogradient coefficient
ε	phase conversion factor
θ	dimensionless temperature field
θ_0	temperature at R=0
θ_1	temperature at R=1
$\tilde{\theta}$	average temperature
λ	latent heat of water evaporation
τ	dimensionless time
ϕ	dimensionless moisture field
ϕ_0	moisture at R=0
ϕ_1	moisture at R=1
$\tilde{\phi}$	average moisture

References

[1] van't Land, C.M. (2011) Drying in the Process Industry. New Jersey: Wiley & Sons.

[2] Mujumdar, A.S. (2015) Handbook of Industrial Drying. fourth ed., Boca Raton: CRC Press.

[3] Strumillo, C. and Kudra, T. (1986) Drying: Principles, Applications and Design. Montreux: Gordon and Breach Science Publishers.

[4] de Vries, D.A. (1958) Simultaneous transfer of heat and moisture in porous media. Transactions of the American Geophysical Union, 39, pp. 909-916.

[5] Luikov, A.V. (1966) Heat and Mass Transfer in Capillary-Porous Bodies. Oxford: Pergamon Press.

[6] Whitaker, S. (1977) Simultaneous heat, mass and momentum transfer in porous media: A theory of drying. Advances in Heat Transfer, 13, pp. 119-203.

[7] Izli, N., Izli, G. and Taskin, O. (2017) Influence of different drying techniques on drying parameters of mango. Food Science Technology, 37, pp. 604-612.

[8] Budd, C.J. and Hill, A.D.C. (2011) A comparison of models and methods for simulating the microwave heating of moist foodstuffs. International Journal of Heat and Mass Transfer, 54, pp. 807-817.

[9] Fennell, L.P. and Boldor, D. (2014) Continuous microwave drying of sweet sorghum bagasse biomass. Biomass & Bioenergy, 70, pp. 542-552.

[10] Song, C., Wang, Y., Wang, S., Cui, Z., Xu, Y. and Zhu, H. (2016) Non-uniformity investigation in a combined thermal and microwave drying of silica gel. Applied Thermal Engineering, 98, pp. 872-879.

[11] Makul, N., Vongpradubchai, S., and Rattanadecho, P. (2018) An experimental study of microwave drying under low pressure to accelerate the curing of Portland cement pastes using a combined unsymmetrical double-fed microwave and vacuum system. International Journal of Heat and Mass Transfer, 127, pp. 179-192.

[12] Si, C., Wu, J., Zhang, Y., Liu, G. and Guo, Q. (2019) Experimental and numerical simulation of drying of lignite in a microwave assisted fluidized bed. Fuel, 242, pp. 149-159.

[13] R.A. Kangarluei. (2015) Heat and mass transfer in industrial biscuit baking oven and effect of temperature on baking time. Journal of Heat and Mass Transfer Research 2, pp.79-90.

[14] Aparecido, J.B. and Cotta, R.M. (1989) Improved one-dimensional fin solutions. Heat Transfer Engineering, 11, pp. 49-59.

[15] Cotta, R.M., Ozisik, M.N. and Mennig, J. (1990) Coupled integral equation approach for phase-change problem in two-regions finite slab. Journal of the Franklin Institute, 327, pp. 225-234.

[16] Cheroto, S., Guigon, S.M.S., Ribeiro, J.W. and Cotta, R.M. (1997) Lumped-differential formulations for drying in capillary porous media. Drying Technology, 15, pp. 811-835.

[17] Corrêa, E.J. and Cotta, R.M. (1998) Enhanced lumped-differential formulations of diffusion problems. Applied Mathematical Modelling, 22, pp. 137-152.

[18] Silva, R.L. (1998) The coupled integral equations approach for the Navier-Stokes equations in three-dimensional laminar flows in rectangular ducts. M.Sc. thesis (in Portuguese), Federal University of Pará, Belém, Brazil.

[19] Reis, M.C.L., Macêdo, E.N. and Quaresma, J.N.N. (2000) Improved lumped-differential formulations in hyperbolic heat conduction. International Communications in Heat and Mass Transfer, 27, pp. 965-974.

[20] Alves, L.S.B., Sphaier, L.A. and Cotta, R.M. (2000) Error analysis of mixed lumped-differential formulations in diffusion problems. Hybrid Methods in Engineering, 2, pp. 409-435.

[21] Su, J. and Cotta, R.M. (2001) Improved lumped parameter formulation for simplified LWR thermohydraulic analysis. Annals of Nuclear Energy, 28, pp. 1019-1031.

[22] Dantas, L.B., Orlande, H.R.B. and Cotta, R.M. (2007) Improved lumped-differential formulations and hybrid solution methods for drying in porous media. International Journal of Thermal Sciences, 46, pp. 878-889.

[23] Naveira, C.P., Lachi, M., Cotta, R.M. and Padet, J. (2009) Hybrid formulation and solution for transient conjugated conduction-external convection. International Journal of Heat and Mass Transfer, 52, pp. 112-123.

[24] Sphaier, L.A. and Jurumenha, D.S. (2012) Improved lumped-capacitance model for heat and mass transfer in adsorbed gas discharge operation. Energy, 44, pp. 978-985.

[25] Cardoso, S.A., Macêdo, E.N. and Quaresma, J.N.N. (2014) Improved lumped solutions for mass transfer analysis in membrane separation process of metals. International Journal of Heat and Mass Transfer, 68, pp. 599-611.

[26] Sphaier, L.A., Su, J. and Cotta, R.M. (2017) Macroscopic heat conduction formulation. In: F.A. Kulacki et al., Eds. Handbook of Thermal Science and Engineering. Chapter 4, Springer International Publishing. [27] Costa Junior, J.M. and Naveira-Cotta, C.P. (2019) Estimation kinetics coefficients in micro-reactors for biodiesel synthesis: Bayesian inference with reduced mass transfer model. Chemical Engineering Research and Design, 141, pp. 550-565.

[28] Hermite, M.Ch. (1878) Sur la formule d'interpolation de Lagrange. Journal Crelle, 84, pp. 70-79.

[29] Conceição, R.S.G., Macêdo, E.N., Pereira, L.B.D. and Quaresma, J.N.N. (2013) Hybrid integral transform solution for the analysis of drying in spherical capillary-porous solids based on Luikov equations with pressure gradient. International Journal of Thermal Sciences, 71, pp. 216-236.

[30] Lu, L. Tang, J. and Liang, L. (1998) Moisture distribution in spherical foods in microwave drying. Drying Technology, 16, pp. 503-528.

[31 Mennig, J., Auerbach, T. and Hälg, W. (1983) Two points Hermite approximation for the solution of linear initial value and boundary value problems. Computer Methods in Applied Mechanics and Engineering, 39, pp. 199-224.

[32] Datta, A.K. (2001) Mathematical modeling of microwave processing of foods: An overview. In: J. Irudayaraj, Ed. Food

Processing Operations Modeling: Design and Analysis. Chap. 6, New York: Marcel Dekker.

[33] Chen, S.D., Singh, R.K, Haghighi, K. and Nelson, P.E. (1993) Finite element analysis of temperature distribution in microwaved cylindrical potato tissue. Journal of Food Engineering, 18, pp. 351-368.

[34] IMSL® (2018) Fortran Numerical Library. Version 2018, Boulder: Rogue Wave Software Inc.

[35] Cotta, R.M. and Ramos, R. (1993) Error analysis and improved formulations for extended surfaces. Proceedings of the NATO Advanced Study Institute on Cooling of Electronic Systems, NATO ASI Series E: Applied Sciences, Turkey June/July, 258, pp. 753-787.